LUND UNIVERSITY

LTH

FACULTY OF ENGINEERING

Biochemical Characterization of CE1 Carbohydrate Esterases with Potential Dual Esterase Activity

Degree Project

Master's Programme in Biotechnology

Division of Biotechnology and Applied Microbiology

Faculty of Engineering (LTH), Lund University

Author: Rithika Vivekananda Nayak

Supervisor: Savvina Leontakianakou

Examiner: Eva Nordberg Karlsson

ACKNOWLEDGEMENT

I would like to sincerely thank my supervisor, Savvina Leontakianakou, for her guidance, patience and continuous support throughout this project. Her encouragement and positivity created a motivating and enjoyable working environment, and her confidence in my abilities helped me grow more confident in my own work. I am also grateful for the welcoming atmosphere she fostered within the group, including the much-appreciated fika clubs.

I would also like to thank my examiner, Eva Nordberg Karlsson, for giving me the opportunity to work on this project and for her valuable ideas and support throughout the study.

My sincere thanks also go to the entire Fermentation Group for their help, discussions, and support during the experimental work. Their presence made the long hours in the lab far less overwhelming and contributed greatly to the overall experience. I would additionally like to thank everyone at the Division of Biotechnology and Applied Microbiology for helping create such a welcoming environment throughout my thesis work.

Finally, I would like to thank my parents and my partner for their constant encouragement and support throughout this journey. Their support has meant a great deal to me during both the challenging and rewarding parts of the work.

ABSTRACT

Carbohydrate esterase family 1 (CE1) enzymes are a diverse group of enzymes involved in plant biomass degradation through removal of acetyl and feruloyl substitutions from polysaccharides. In this study, several putative CE1 enzymes were characterized to find out their substrate preference, catalytic properties and possible role during biomass hydrolysis. Functional screening using *p*NP-acetate and *p*NP-ferulate showed clear differences between the analyzed enzymes. AXE2 and FAE9 were active toward both substrates, whereas ACE3 showed lower activity and appeared to hydrolyze acetyl ester substrates. Kinetic analysis showed differences between AXE2 and FAE9, where AXE2 showed stronger affinity toward ferulate (K_m = 0.821±0.127 mM), while FAE9 displayed higher catalytic turnover and catalytic efficiency toward *p*NP-acetate, with a k_{cat} of 37.414 ± 3.217 min^{-1} and catalytic efficiency of 43.692 ± 3.495 $mM^{-1}min^{-1}$. The hydrolysis experiments performed with the GH11 xylanase Pentopan Mono BG resulted in noticeable changes in oligosaccharide profiles across several biomass substrates, particularly for arabinoxylan and xylan-rich substrates, suggesting possible synergy between the CE1 enzymes and the GH11 xylanase during biomass degradation. Hence, the findings agree with the proposed accessory role of CE1 enzymes in biomass hydrolysis and provide insight into their possible use in enzymatic biomass conversion systems.

TABLE OF CONTENTS

1. INTRODUCTION

1.1 Plant Biomass and Structural Complexity

Plant biomass, primarily composed of lignocellulosic material, is a major renewable resource for the production of biofuels and other value-added products. However, the efficient utilization of plant biomass is limited by the structural complexity of the plant cell wall. (Yang et al., 2024)

The cell wall is a highly complex structure mainly composed of cellulose, hemicellulose and lignin as seen in **Figure 1** (Brethauer et al., 2020). Cellulose consist of β -1,4 D - glucose units and exists as tightly packed, crystalline microfibrils that provide mechanical strength and forms the structural backbone of the plant cell wall (Collard et al., 2014; Brethauer et al., 2020). Encasing these microfibrils is hemicellulose, which is a collection of heterogeneous branched polysaccharides. Xylan is the most abundant type in hardwoods and cereals, with a backbone composed of β -1,4 D - xylose moieties. Xylan can interact with the surfaces of the cellulose fibers and contributes in the formation of a supportive matrix (Collard et al., 2014). The gaps within this carbohydrate matrix are occupied by lignin, an aromatic polymer forming a sturdy and water-repellent barrier (Brethauer et al., 2020).

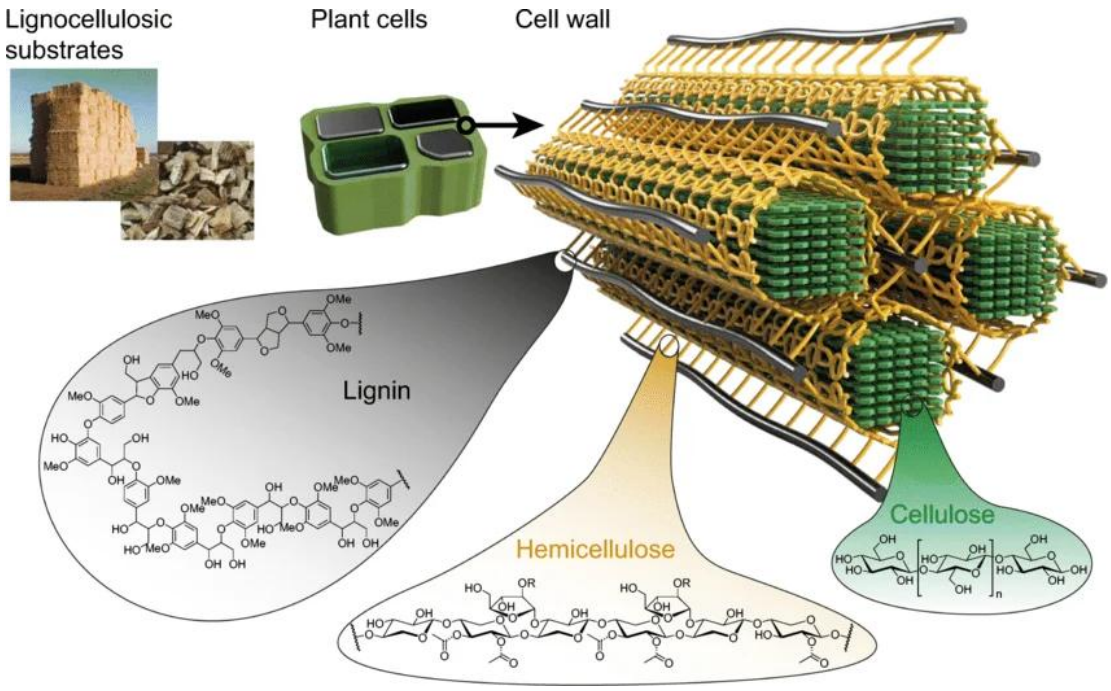

Figure 1: Structural organisation of plant cell walls showing the arrangement of cellulose, hemicellulose and lignin. (Brethauer et al., 2020)

Additionally, the hemicellulose is often decorated with ester-linked substituents, including acetyl groups and hydroxycinnamic acids such as ferulic acid (Yoshimi et al., 2024; Leontakianakou et al., 2025). These decorations enhance the biomass recalcitrance by forming cross-links between hemicellulose and lignin and sterically hindering enzymatic access to glycosidic bonds (Leontakianakou et al., 2025). Hence, the efficient hydrolysis of plant biomass requires the removal of these ester-linked modifications (Yoshimi et al., 2025).

1.2 Carbohydrate Esterases and the CE1 family

Carbohydrate esterases are essential for the breakdown of plant biomass as they catalyse the hydrolysis of ester-linked groups from polysaccharides and lignocellulosic materials (Armendáriz-Ruiz et al., 2018). The CE1 family, classified in the Carbohydrate-Active enZymes (CAZy) database, is one of the most functionally diverse groups within the carbohydrate esterases (Drula et al., 2021; Nakamura et al., 2017).

CE1 enzymes show a wide range of functions including acetyl xylan esterases (AXE), feruloyl esterases (FAE), acetyl esterase, carboxylic ester hydrolase, trehalose 6-O-mycolyltransferase and diacylglycerol O-acyltransferase (CAZy database., 2026). This functional diversity is a reflection of their ability to act on a variety of substrates across different biological circumstances, ranging from microbial metabolism to plant cell wall modifications (Nakamura et al., 2017).

1.3 Functional Activities of CE1 Esterases: AXEs and FAEs

Within the CE1 esterases, the two major functional activities are acetyl xylan esterases (AXEs) and ferulic acid esterases (FAEs), which have differing substrate specificity and functional roles in biomass degradation (Dilokpimol et al., 2022; Phienluphon et al., 2022).

Acetyl xylan esterases (AXEs) hydrolyse acetyl groups attached to hemicellulosic polysaccharides, particularly xylan as seen in **Figure 2**. Since these substitutions can hinder the activity of glycoside hydrolases, by removing these groups, the AXEs reduce the steric hindrance and increase the accessibility of hemicellulose to enzymatic degradation (Alalouf et al., 2011; Dilokpimol et al., 2022).

In contrast, the ferulic acid esterases (FAEs) target ester linkages between hydroxycinnamic acids such as ferulic acid and polysaccharides as shown in **Figure 2** (Wu et al., 2016). These feruloyl groups strengthen the plant cell wall structure by cross-linking hemicellulose to lignin. The FAEs disrupt these cross-links, loosening the lignocellulosic network and facilitating the breakdown of biomass (Phienluphon et al., 2022).

Although AXEs and FAEs perform distinct functions, the distinction between these activities within the CE1 family is not always clearly defined, as some enzymes may exhibit overlapping or dual functionality (Dilokpimol et al., 2022)

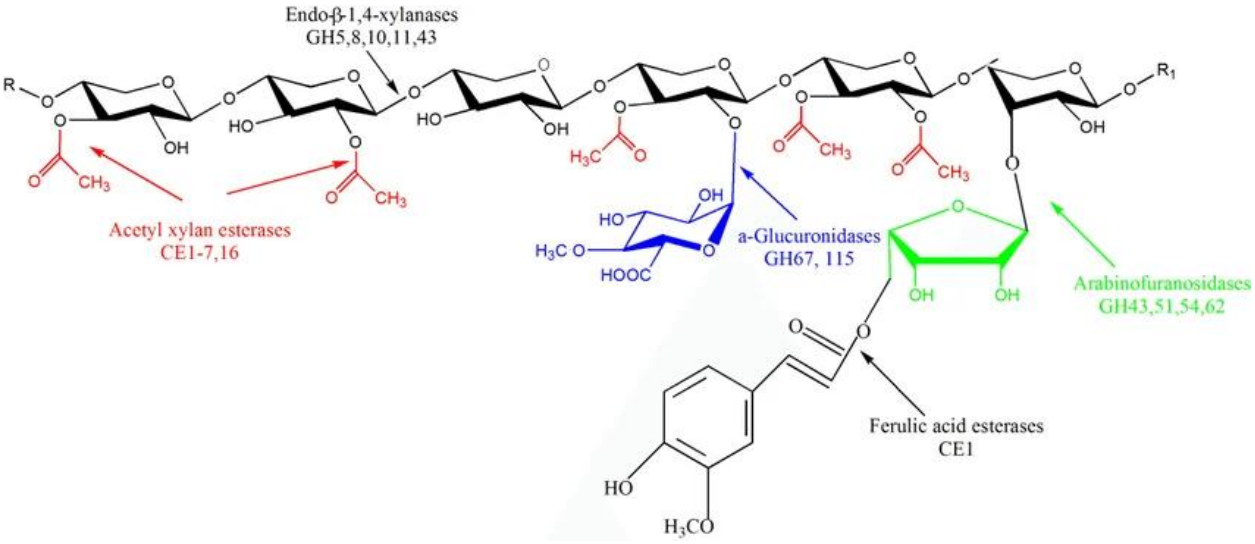

Figure 2: Structure of xylan, showing all modifications including the acetyl and feruloyl group. The arrows mark the enzyme activities involved in their removal (Wu et al., 2016)

1.4 Biotechnological Applications of CE1 Esterases

CE1 esterases are particularly interesting in biotechnology due to their role in overcoming biomass recalcitrance (Armendáriz-Ruiz et al., 2018). These enzymes facilitate the removal of ester-linked substitutions, thereby improving the enzymatic degradation of lignocellulosic biomass for the production of biofuels and bio-based chemicals (Grippi et al., 2020; Oliveira et al., 2019). Additionally, CE1 enzymes contribute to improved digestibility and the release of valuable phenolic compounds in the food and feed industries (Chowdhury et al., 2025). Hence, a detailed understanding of their activity and substrate specificity is essential for optimizing enzyme systems for industrial applications.

1.5 Knowledge Gap in CE1 Functional Characterization

With the increasing number of annotated CE1 enzymes, their biochemical characterization remains limited (Nakamura et al., 2017). Due to limited experimental confirmation of their catalytic properties, many members of this family are assigned hypothesized roles based mainly on sequence similarities (Mäkelä et al., 2018).

Determining substrate specificity within the CE1 family is a significant challenge. The feruloyl esterase (FAE) and acetyl xylan esterase (AXE) are usually linked to certain enzymes, but it is not always evident how these functions differ from one another (Li et al., 2020). Specifically, it is still unclear if some CE1 enzymes have dual activity toward both feruloyl and acetyl substrates or strict selectivity (Dilokpimol et al., 2022).

2. AIM OF THE STUDY

The aim of this study is to recombinantly produce and functionally characterize selected CE1 carbohydrate esterases through activity and kinetic analysis using feruloyl and acetyl model substrates in order to determine whether the enzymes exhibit feruloyl esterase (FAE), acetyl xylan esterase (AXE) or dual activity. In addition, the enzymes were evaluated on different complex polysaccharide substrates to assess their functionality and specificity.

3. MATERIALS AND METHODS

3.1 Recombinant Production of CE1 Enzymes

3.1.1 Transformation of Expression Strains

Escherichia coli BL21(DE3) cells were individually transformed with six plasmids, shown in **Table 1,** encoding selected CE1 enzymes provided by the research group. The transformed cells were plated on LB agar plates containing ampicillin and incubated overnight at 37℃. Single colonies obtained after incubation were streaked onto fresh LB-ampicillin plates to prepare mother plates, which were subsequently used for recombinant protein expression experiments.

Table 1: Plasmids used for the transformation of *E.coli* BL21(DE3) cells.

Organism	In house designation	Molecular Weight (kDa)
Algoriphagus terrigena	AXE2	33
Ruminiclostridium cellulolyticum	AXE4	53
SINTEF selection	ACE3	32
	ACE5	33
	FAE7	37
	FAE9	34

3.1.2 Protein Expression and Purification

For recombinant protein expression, a single colony from each mother plate was inoculated into 3 ml LB medium containing ampicillin and incubated overnight at 37 ℃ as a pre-inoculum culture. 1 mL of the pre-inoculum was transferred into 100 mL LB medium supplemented with ampicillin and incubated at 37 ℃. Cell growth was monitored by measuring the optical density at 600 nm (OD600nm) and protein expression was induced with 1mM IPTG once the cultures reached an OD_{600nm} of 0.6-0.8.

Following the induction, the cultures were incubated under two different conditions, at 16 ℃ overnight or at 26 ℃ for 4 h. Cells were subsequently harvested by centrifugation at 9880 xg for 15 minutes at 4℃ and the resulting pellets were collected for protein purification.

The cell pellets were resuspended in HEPES binding buffer containing 50 mM HEPES, 500 mM NaCl, 50 mM imidazole and 5 % (v/v) glycerol. Cell lysis was performed by sonication for 5

minutes at 30 % amplitude. The lysates were then centrifuged at 20200 xg for 30 min at 4 ℃ and the supernatants containing the soluble protein were collected.

Protein purification was carried out using an ÄKTA purification system, using 1 mL HisTrap affinity column for purification of the His-tagged CE1 proteins. The HEPES binding buffer and HEPES elution buffer containing 50 mM HEPES, 500 mM NaCl and 500 mM imidazole were used. Purified proteins were then dialyzed overnight, using a dialysis membrane against PBS buffer.

3.1.3 SDS-PAGE Analysis and Protein Quantification

SDS-PAGE analysis was performed at different stages of protein production and purification to assess protein expression and purity. Before purification, samples from the total fraction obtained after sonication and the soluble fraction collected after centrifugation were analyzed. Additional SDS-PAGE analyses were carried out after ÄKTA purification, both before and after dialysis.

Protein concentration was determined using the Bradford assay. Absorbance was measured at 595 nm and protein concentrations were calculated using a with bovine serum albumin (BSA) standard curve.

3.2 Functional Characterization of CE1 Enzymes

3.2.1 *p*-nitrophenol **(*p*NP) Activity Assay**

The activity of the CE1 enzymes was evaluated using the model substrates *p*NP-acetate and *p*NP-ferulate. A standard curve was drawn from known *p*NP concentrations.

The reaction mixture consisted of 75 µL milli-Q water, 100 µL buffer, 10 µL substrate solution and 5 µL enzyme solution (0.3-1.2 g/L) in the microplate wells. All reactions were performed in triplicate. The assay plates were incubated at 40 ℃ and absorbance was measured at 410 nm.

Both *p*NP-acetate and *p*NP-ferulate were initially prepared in a 1:1 mixture of acetonitrile and isopropanol. Lower solubility of *p*NP-ferulate was seen under these conditions, due to which optimization was performed, and it is discussed in section 3.2.2 Enzyme Kinetics.

3.2.2 Stability Analysis

Enzyme stability was evaluated over approximately twenty days by measuring activity against *p*NP-acetate and *p*NP-ferulate at various time points. The assays were carried out using 10 mM substrate solutions and the PBS buffer was used. Stability was assessed based on the release of *p*NP during hydrolysis.

The enzymes were stored at 4 °C between measurements. For each stability analysis, the same enzyme batch was used throughout the experiment, and the analysis was repeated using different purified enzyme batches. All reactions were performed in triplicate.

3.2.3 Enzyme Kinetics

Enzyme kinetics were evaluated using different concentrations of the *p*NP-acetate (0-5 mM) and *p*NP-ferulate substrates (0-2mM). Due to the lower solubility of *p*NP-ferulate under the initial assay conditions, optimization of solvent composition, buffer system, pH and DMSO concentration was performed prior to kinetic analysis. The assays were performed with PBS and McIlvaine buffer, at pH 7 for *p*NP-acetate and *p*NP-ferulate assays, respectively. *p*NP-acetate was resuspended in 1:1 acetonitrile: isopropanol, *p*NP-ferulate was prepared in 80% DMSO. All reactions were carried out in triplicate.

For each substrate concentration, the release of *p*NP was monitored over time, and plots of *p*NP concentration over time were generated. The initial reaction velocity [V] was determined from the slope of the early linear portion of each reaction curve.

The calculated initial rates were then plotted against substrate concentration [S], and the Michaelis-Menten equation was applied to determine the kinetic parameters, using the Root Mean Square Error (RMSE) in non-linear regression with Excel.

$$V = \frac{Vmax\ [S]}{Km + [S]}$$

where V represents the reaction velocity, [S] the substrate concentration, V_{max} the maximum reaction velocity and K_m the Michaelis constant. Standard deviations were calculated from triplicate measurements.

3.3 NanoDSF Analysis

Nano differential scanning fluorimetry (NanoDSF) was performed to evaluate the thermal stability of the dialyzed purified CE1 enzymes under different pH conditions. The enzyme concentration was adjusted to a final concentration of 0.2 g/L based on protein concentrations determined using the Bradford assay. McIlvaine buffer was used for all measurements, with pH conditions of 3.2, 4.4, 5.6, 6, 6.4, 7, 7.5, 8 and 8.9

3.4 Analysis on Complex Polysaccharide Substrates

3.4.1 Complex Substrate Reaction

Complex substrate reactions were performed using seven different substrates, shown in **Table 2,** to evaluate CE1 enzyme activity on complex substrates. Each reaction mixture contained a final substrate concentration of 0.5%, a final CE1 enzyme concentration of 0.1 g/L. Pentopan Mono BG is a GH11 endoxylanase and was added from a 10g/L stock solution to a final concentration of 19µL/mL, simultaneously with the CE1 enzymes to assess the possibility of synergistic degradation. The remaining reaction volume consisted of the appropriate buffer, based on the nanoDSF results. The enzymes and their respective optimal conditions are summarized in **Table 2.** All reactions were carried out in duplicate.

In addition to the complete reaction mixtures, two control conditions were prepared for each substrate, one without the CE1 enzyme and another without both the CE1 enzyme and the Pentopan Mono.

Samples from reactions containing both enzymes were collected at time points 0h, 1h, 6h, 24h and 48h. Control reactions were sampled at 0h and 48h. All collected samples were stored at -20℃ prior to further analysis.

Table 2: Enzyme-specific reaction conditions for complex biomass substrate analysis

CE1 Enzyme	pH	Temperature (℃)	Complex Polysaccharides	Supplier
AXE2	6.4	40℃	1. Larch Arabinogalactan	Megazyme
			2. Wheat Arabinoxylan (Low Viscocity)	Megazyme
			3. Rye Arabinoxylan	Megazyme
			4. Arabinan-Sugar Beet	Megazyme
FAE9	6	50℃	5. Acetylated Xylan-Birchwood	Sigma-Aldrich
			6. Beechwood Xylan	Sigma-Aldrich
			7. Acacia Gum	

3.4.2 HPLC Analysis

HPLC analysis was performed using a Vanquish HPLC system to monitor the release of ferulic acid from complex polysaccharide substrate reactions. Prior to reactions, the samples were diluted (x10) in Milli-Q water and filtered through 0.2μM filters into HPLC vials. Ferulic acid standards of different concentrations (0.1-100 μM) were also prepared to identify and quantify ferulic acid release.

Separation was carried out using a Kinetex 2.6 μm Biphenyl 100 Åcolumn, 50 x 2.1 mm, with AJ0-9209 BP pre-column. The mobile phase consisted of Eluent A: methanol, acetic acid and Milli-Q in a ratio of 10:2:88, and Eluent B: methanol, acetic acid and Milli-Q in a ratio of 90:2:8. The elution performed isocratically with 13 % B, for a total run time of 12 min. Detection was performed at 280 nm with a flow rate of 0.3mL/min.

3.4.3 HPAEC-PAD Analysis

High-performance anion exchange chromatography with pulsed amperometric detection (HPAEC-PAD) was used to evaluate release of xylo-oligosaccharides generated enzymatic hydrolysis of complex substrates. Prior to analysis, the samples were diluted (50x) in milli-Q water and filtered through 0.2 μM filters into HPAEC-PAD vials. Standards consisting of xylobiose, xylotriose, xylotetrose, xylopentose and xylohexose were prepared at different concentrations and used for peak identification.

All analyses were carried out using a Dionex ISC 6000 system (Thermo Fisher Scientific, Waltham, USA) equipped with a CarboPac PA200 analytical column (250 mm x 3 mm, 5.5 μm particle size) and corresponding guard column (50mm x 3 mm). Separation was achieved using three mobile phases designated as A, B and C consisting of milli-Q water, NaOH supplemented with NaOAc, and NaOH, respectively. The total run time for each analysis was 23 min.

4. RESULTS

4.1 Recombinant Production and Purification of CE1 Enzymes

4.1.1 Transformation

Transformation was successful for most of the CE1 candidates tested under initial conditions. One candidate required optimization of the transformation conditions, including changes in the amount of plasmid DNA and competent cells, before successful transformants were obtained. The transformation outcomes for all candidates are summarized in **Table 3.**

Table 3: Transformation outcomes for CE1 enzyme candidates

	AXE 2	AXE 4	ACE 3	ACE 5	FAE 7	FAE 9

Transformation 1	☑	✗	☑	☑	☑	☑
Volume of competent cells (µL)	**50**	**50**	**25**	**25**	**25**	**25**
Volume of plasmid (µL)	**2**	**2**	**1**	**1**	**1**	**1**
Transformation 2	-	☑	-	-	-	-
Volume of competent cells (µL)	-	**25**	-	-	-	-
Volume of plasmid (µL)	-	**1**	-	-	-	-

4.1.2 Protein Expression

SDS-PAGE analysis of the total fraction (TF) and the soluble fraction (SF) showed protein bands at the expected molecular weight for all six CE1 enzyme candidates. Protein expression was initially evaluated at both 16 ℃ and 26 ℃ following IPTG induction. Expression at 26 ℃ resulted in clearer soluble protein bands, which is seen in **Figure 3**, and was therefore selected for future experiments.

AXE2 and AXE4 showed stronger bands in the soluble fractions, while ACE3 showed clear but comparatively less intense bands. ACE5, FAE7 and FAE9 showed weaker bands but still indicated soluble protein expression.

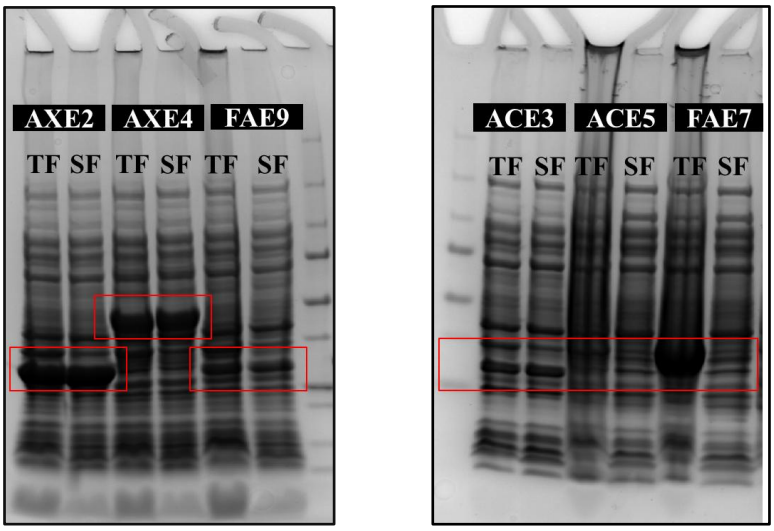

Figure 3: SDS-PAGE analysis of recombinant CE1 enzyme expression in total fraction (TF) and soluble fraction (SF) samples

4.1.3 Protein Purification

SDS-PAGE analysis of the purified protein before and after dialysis showed bands at the expected molecular weights for most candidates as seen in **Figure 4.** AXE2, AXE4, ACE3 and FAE9 showed stronger bands following purification and dialysis.

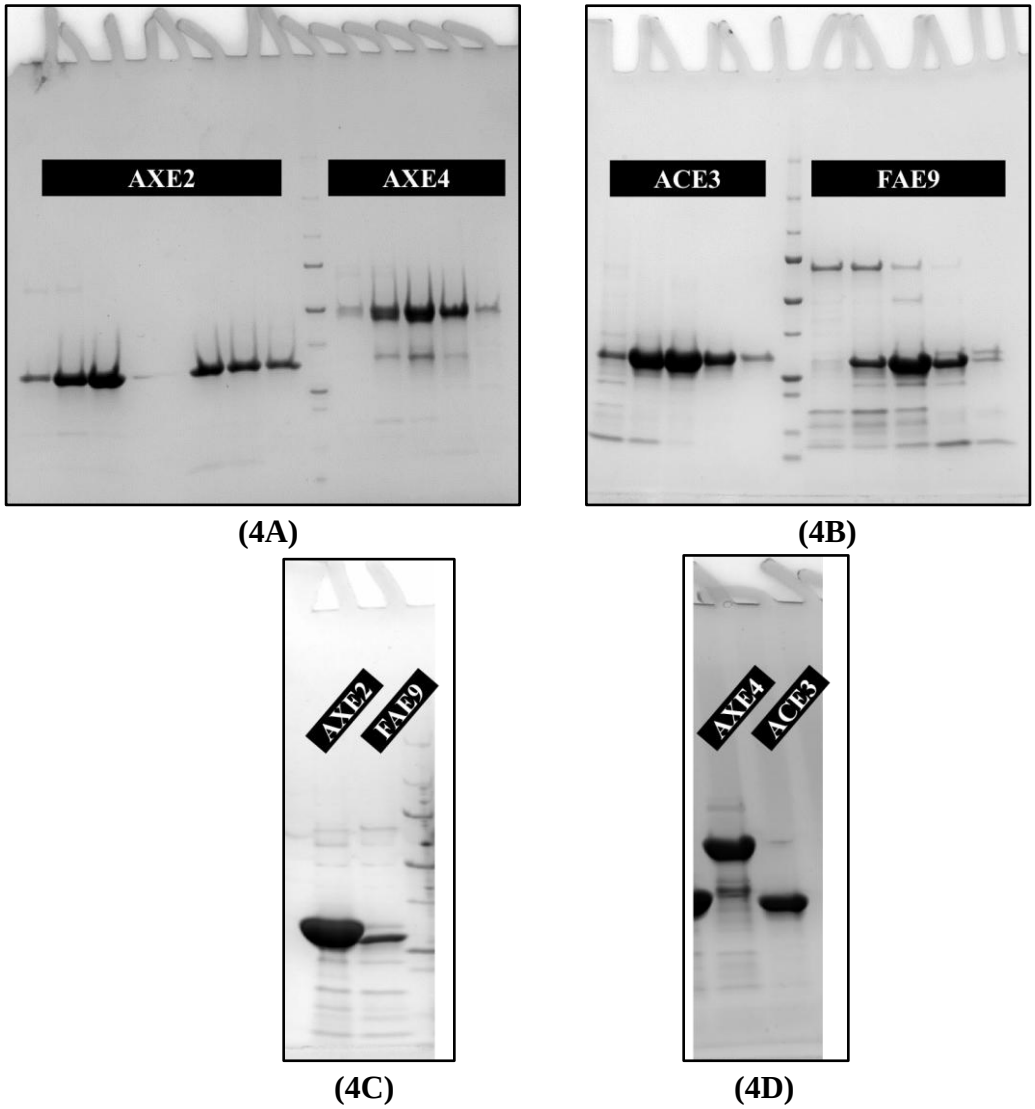

(4A) **(4B)**

(4C) **(4D)**

Figure 4: SDS-PAGE analysis of purified and dialyzed CE1 enzymes selected for characterization. (4A) Purified AXE2 and AXE4 samples, (4B) purified ACE3 and FAE9 samples, (4C) dialyzed AXE2 and FAE9 samples, (4D) dialyzed AXE4 and ACE3 samples.

In contrast, ACE5 and FAE7 showed weaker bands that did not align well with the expected molecular weights, as seen in **Figure 5,** and were therefore not selected for characterization.

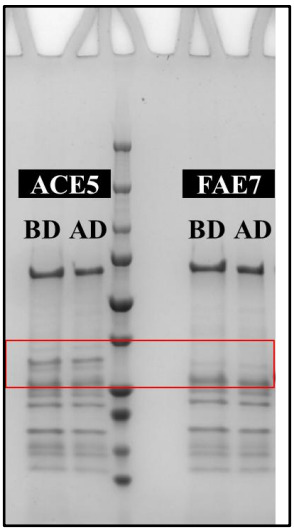

Figure 5: SDS-PAGE analysis of purified and dialyzed ACE5 and FAE7 samples. BD: before dialysis, AD: after dialysis.

4.1.4 Protein Quantification

Protein concentrations varied between the purified enzymes following dialysis. AXE2, AXE4, ACE3 and FAE9 showed sufficient protein concentrations for subsequent characterization, which are summarized in **Table 4.** The Bradford standard curve used for protein quantification is provided in **Appendix Figure A1 and Table A1.**

Table 4: Protein concentrations of purified CE1 enzymes

Enzyme	Protein Concentration (g/L)
AXE2	1.24
AXE4	0.93
ACE3	0.54
FAE9	0.32

4.2 Functional Screening of CE1 Enzymes

Differences in substrate activity were detected among the selected enzymes when tested on *p*NP-acetate and *p*NP-ferulate substrates (**Figure 6**). AXE2 and FAE9 showed activity toward both substrates. AXE4 showed greater activity toward *p*NP-acetate, while only low activity was present toward *p*NP-ferulate. Similarly, ACE3 showed activity toward *p*NP-acetate, with almost no activity detected toward *p*NP-ferulate. The substrate activities are summarized in **Table 5.**

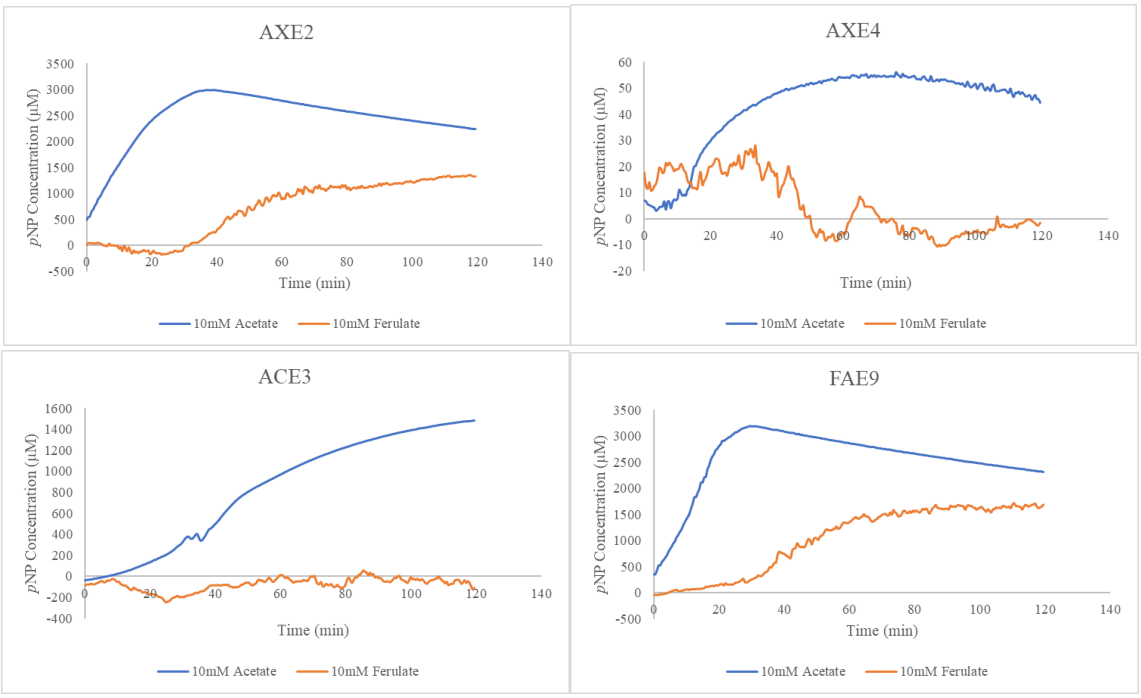

***Figure 6**:* Screening of AXE2, AXE4, ACE3 and FAE9 enzymes using *p*NP-acetate and *p*NP-ferulate substrates. The *p*NP-ferulate graphs shown are prior to substrate resuspension optimization

Table 5: Functional screening results of CE1 enzymes on model *p*NP substrates

Enzyme	***p*NP-acetate**	***p*NP-ferulate**
AXE2	Present	Present
AXE4	Low	Low
ACE3	Moderate	Absent
FAE9	Present	Present

4.3 Stability Analysis of CE1 Enzymes

Relative activity measurements over approximately 20 days showed that AXE2 and FAE9 retained most of their activity on both *p*NP-acetate and *p*NP-ferulate substrates throughout the analysis period (**Figure 7**). There was only a slight decrease in activity over time.

AXE4 and ACE3 also retained activity on *p*NP-acetate across the storage period, with a gradual decrease in activity over time. While activity measurements were also performed using *p*NP-ferulate for these enzymes, the activity levels were too low for reliable interpretation.

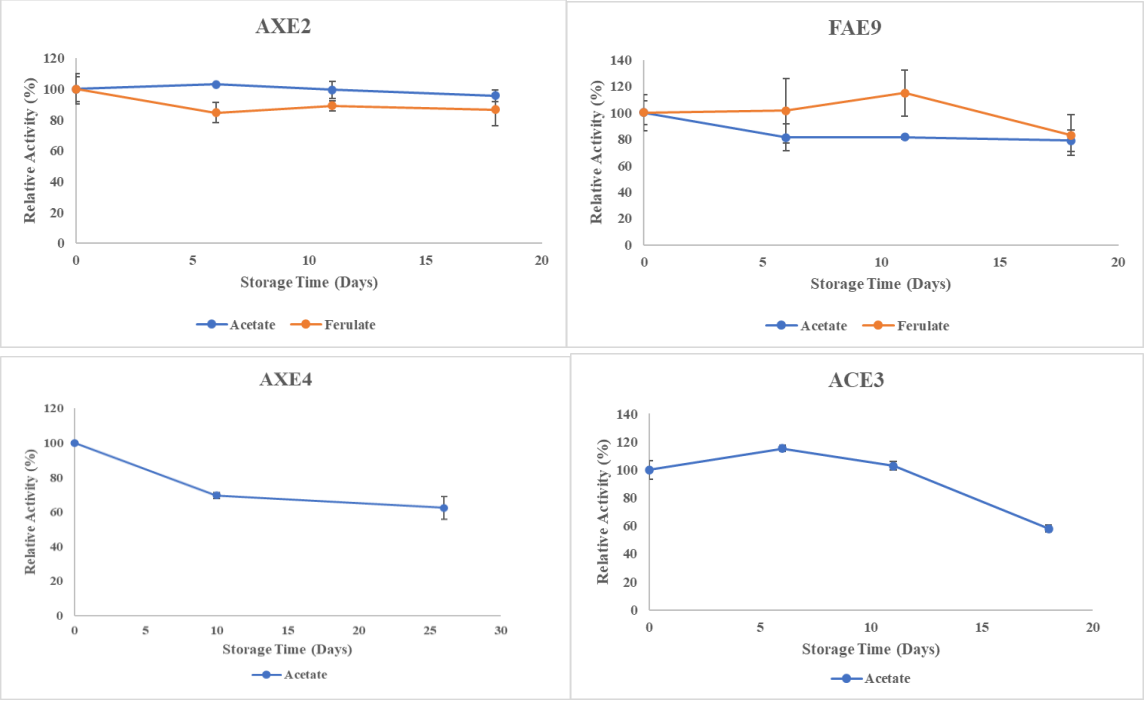

Figure 7: Stability analysis of CE1 enzymes over approximately 20 days based on relative activity on *p*NP substrates

4.4 Kinetic Characterization of CE1 Enzymes

Initial experiments using *p*NP-ferulate showed limited substrate solubility under the original assay conditions. Optimization of the solvent composition, buffer system, pH and DMSO concentration improved substrate solubility and assay consistency for subsequent kinetic analyses. The final conditions selected for *p*NP-ferulate kinetics consisted of McIlvaine buffer at pH 7 with the substrate prepared in 80% DMSO.

Kinetic analysis was carried out for AXE2 and FAE9 using both *p*NP-acetate and *p*NP-ferulate substrates, while ACE3 was analyzed using *p*NP-acetate only. AXE4 was not taken forward for kinetic characterization due to difficulties in protein production and the low activity during functional screening.

Michaelis-Menten kinetics were obtained for the selected enzymes using the corresponding *p*NP substrates. The calculated kinetic parameters are summarized in **Table 6**. Representative Michaelis-Menten plots for the selected CE1 enzymes are provided in Appendix Figure A4.

Table 6: Kinetic parameters of selected CE1 enzymes determined using *p*NP substrates (n = 3)

Enzyme	Substrate	K_m ± SD (mM)	V_{max} ± SD (µM/min)	k_{cat} ± SD (min^{-1})	Catalytic efficiency ($mM^{-1}min^{-1}$)

AXE2	*p*NP-acetate	1.047 ± 0.22	365.52 ± 22.564	9.7 ± 0.573	9.635 ± 2.576
	*p*NP-ferulate	0.821 ± 0.127	171.551 ± 15.252	4.562 ± 0.406	5.589 ± 0.368
FAE9	*p*NP-acetate	0.856 ± 0.012	352.07 ± 30.272	37.414 ± 3.217	43.692 ± 3.495
	*p*NP-ferulate	1.04 ± 0.046	233.397 ± 6.7	24.803 ± 0.712	23.886 ± 1.24
ACE3	*p*NP-acetate	3.475 ± 0.757	155.15 ± 21.37	9.18 ± 1.265	2.676 ± 0.238

4.5 NanoDSF Analysis

Previously obtained NanoDSF results showed that AXE2 had preferred a pH of 6.4 and AXE4 showed a preferred pH of 5.6. Both enzymes worked well at 40 ℃.

NanoDSF analysis was additionally carried out for ACE3 and FAE9, and the optimum pH and temperature conditions for these enzymes are summarized in **Table 7.**

Table 7: NanoDSF Analysis for ACE3 and FAE9 (n=2)

pH	**Temperature (**℃)	
	ACE3	**FAE9**
3.2	ND	26.45 ± 0.05
4.4	55.3 ± 1.4	53 ± 0.0
5.6	**63.95 ± 0.15**	63.1 ± 0.0
6	63.3 ± 0.1	**63.9 ± 0.1**
6.4	61.7 ± 0.0	63.45 ± 0.05
7	60.7 ± 0.1	61.7 ± 0.0
7.5	59.2 ± 0.0	59.7 ± 0.0
8	58.7 ± 0.0	57.9 ± 0.0
8.9	54.8 ± 0.1	55.55 ± 0.05

4.6 Activity on Complex Substrates

4.6.1 HPLC Analysis

HPLC analysis was carried out to detect the release of ferulic acid and related compounds following enzymatic hydrolysis of the complex substrates. However, no clear peaks corresponding to the target compounds were present in the chromatograms.

This was most likely due to the samples being overly diluted prior to analysis, resulting in concentrations below the detection range of the method. Therefore, no comparison between the different treatment conditions could be made based on the obtained chromatograms.

4.6.2 HPAEC-PAD Analysis

Table 8: HPAEC-PAD chromatograms showing the hydrolysis profiles of different complex polysaccharide substrates following treatment with Pentopan Mono BG (PP) alone and in combination with the CE1 enzymes (PP + Enz). Chromatograms include standards, control samples, PP-treated samples, PP + enzyme samples at t=0 h and PP + enzyme samples at t=48 h. Peaks corresponding to xylo-oligosaccharide standards are labelled as X2-X6, representing xylobiose, xylotriose, xylotetrose, xylopentose and xylohexose, respectively. Additional peaks were labelled alphabetically (A-E) for comparison of changes between treatment conditions. Corresponding peak area values are provided in Appendix Table A3.

AXE2

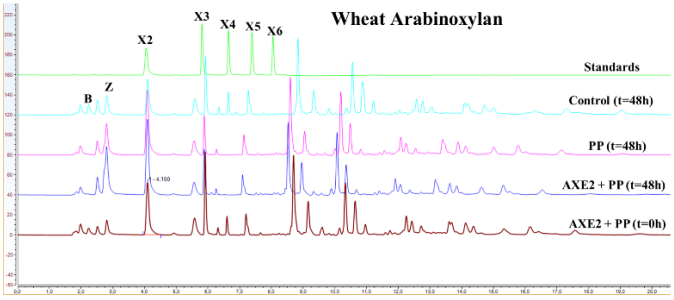

- X2 is higher in PP + AXE2 (t=48h) compared to PP alone.
- Initial peaks, probably corresponding to monosaccharides increases following enzyme treatment.
- X3 decreased in the enzyme treated samples.
- Peak B was absent in the PP and PP + AXE2 samples.
- Slight shift in retention times after 7 min.

FAE9

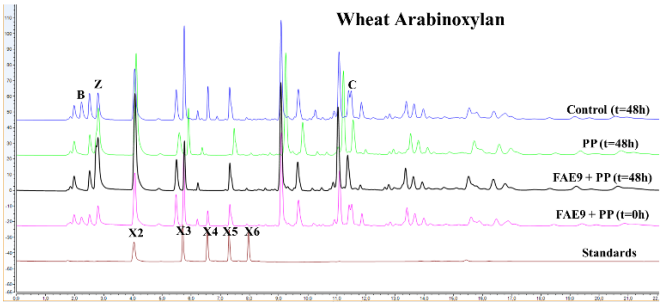

- Initial peaks, probably corresponding to monosaccharides increased following enzyme treatment.
- Higher X2 peak was seen in PP and PP + FAE9(48h).
- X3 decreased in the enzyme treated samples.
- Peak B was absent in PP and PP + FAE9 (48h) samples.
- Peak C changed from a split peak to a single peak following enzymatic treatment.

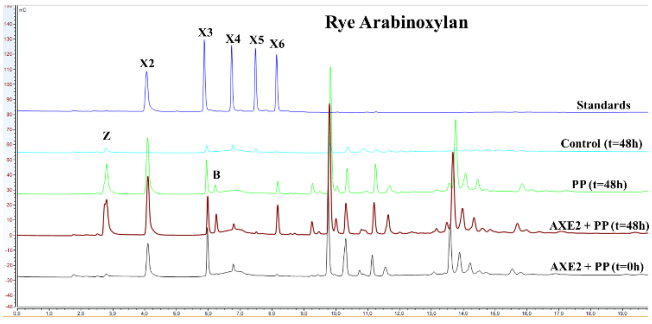

- Peak Z and X2 showed higher peak areas in the PP + AXE2 (t=48h) sample.
- X3 decreased in the PP and PP + AXE2 (48h), compared to PP + AXE2 (0h).
- X6 and additional peaks adjacent to X3 detected following enzymatic treatment.

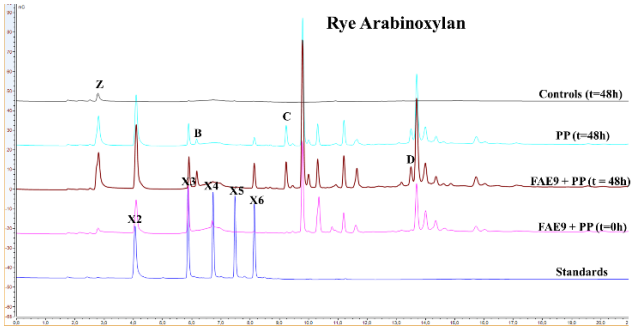

- Higher Peak Z, X2 and X6 peak areas were observed in PP + FAE9 (48h) sample.
- X3 decrease in the presence of enzymes.
- Additional peaks B, C and D were observed only in enzyme treated samples.

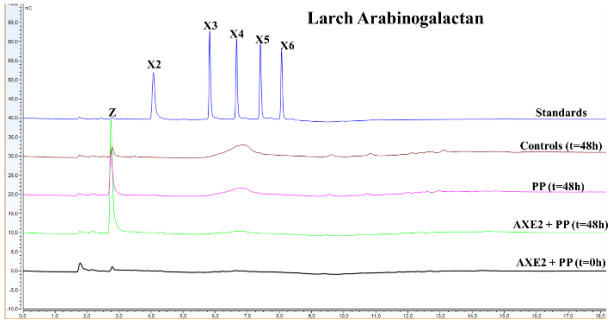

- Peak Z, increased in enzymatic samples, with a higher peak area in PP + AXE2 (48h).

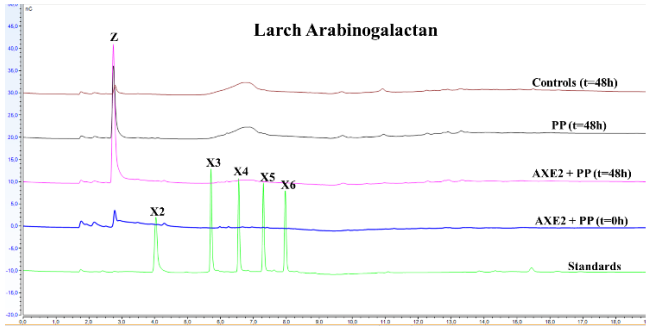

- Peak Z, increased in enzymatic samples, with a higher peak area in PP + FAE9 (48h).

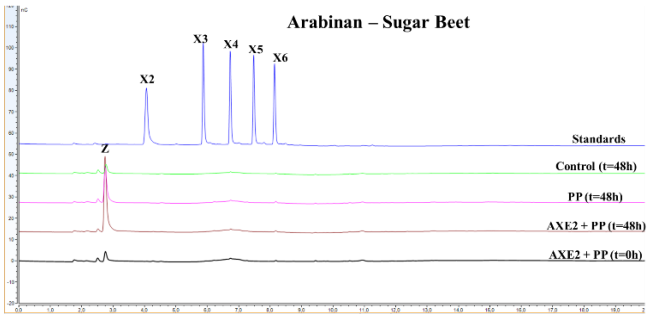

- Peak Z, increased in enzymatic samples, with a higher peak area in PP + AXE2 (48h).

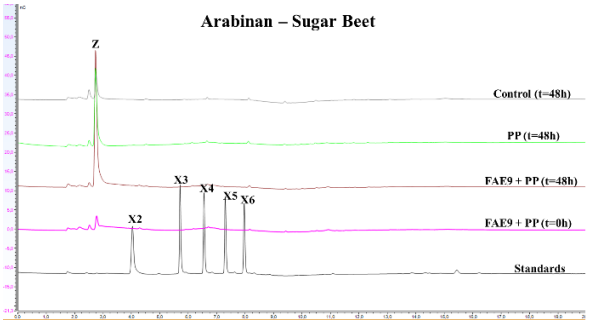

- Peak Z, increased in enzymatic samples, with a higher peak area in PP + FAE9 (48h).

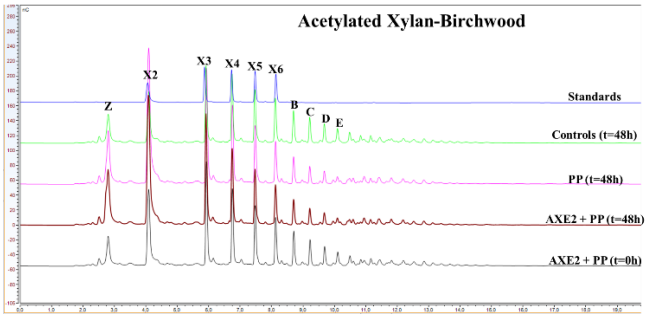

- Peak Z, X2 and X3 showed higher peak areas in PP + AXE2 (48h) sample.
- X4-X6 showed a decrease in enzyme treated samples.
- Additional late-eluting samples (B-E) also showed decreasing trends following enzymatic treatment.

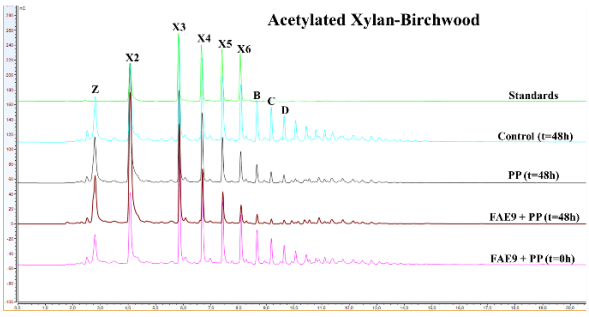

- Peak Z and X2 showed higher peak areas in the PP + FAE9 (48h) sample.
- X4-X6 and additional late-eluting peaks (B-D) showed decreasing trends following enzymatic treatment.

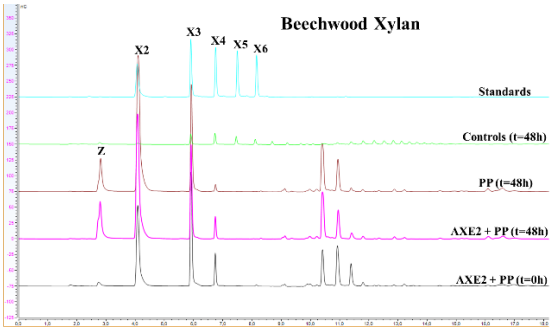

- Peak Z and X2 showed substantially higher peak areas in the enzyme-treated samples.
- X3 and X4 showed lower peak areas following enzyme treatment
- The changes in peak areas were more pronounced in PP compared to PP + AXE2 (48h).

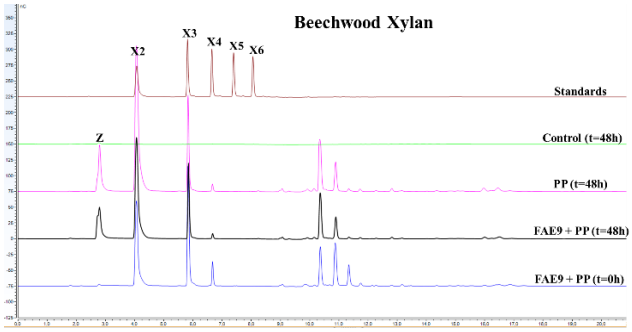

- Peak Z and X2 showed substantially higher peak areas in the enzyme-treated samples.
- X3 and X4 showed lower peak areas following enzyme treatment
- The changes in peak areas were more pronounced in PP compared to PP + FAE9 (48h).

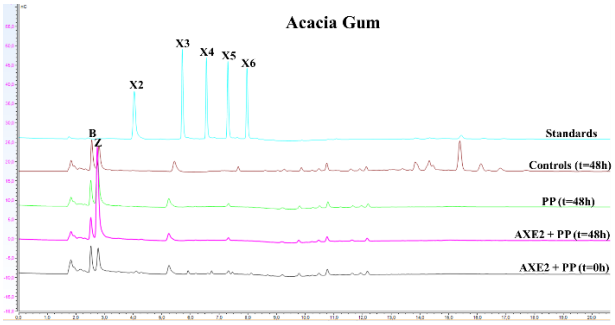

- Peak Z showed higher peak areas in the enzyme-treated samples, with the highest value observed in the PP + AXE2 (48h) sample.
- Peak B showed a slight decrease following enzymatic treatment.

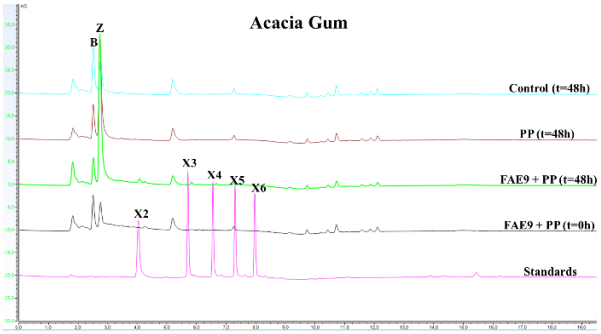

- Peak Z showed higher peak areas in the enzyme-treated samples, with the highest value observed in the PP + FAE9 (48h) sample.
- Peak B showed a slight decrease following enzymatic treatment.

5. DISCUSSION

5.1 Recombinant Protein Production and Functional Screening

Most of the selected CE1 candidates were successfully transformed and expressed under the tested conditions, but the expression levels and purification profiles varied between the enzymes. AXE2 and AXE4 showed strong expression with clear bands close to the expected molecular weights, while ACE3 showed comparatively lower but still detectable expression.

ACE5 and FAE7 showed weaker expression and the purified bands did not fully match the expected molecular weights. This may indicate protein degradation, reduced stability or improper folding during recombinant expression in *E.coli* (Francis et al., 2010; Baneyx et al., 1999). Based on these observations, both enzymes were excluded from characterization.

The functional screening assays also revealed certain dissimilarities in substrate preference among the enzyme candidates. AXE2 and FAE9 hydrolyzed both *p*NP-acetate and *p*NP-ferulate, and AXE4 and ACE3 showed noticeably stronger activity toward *p*NP-acetate, when compared to very limited activity toward *p*NP-ferulate. This may reflet that these enzymes prefer acetyl ester hydrolysis. Even though AXE4 and ACE3 showed higher activity toward *p*NP-acetate, the activity of ACE3 was significantly lower than that of AXE2 and FAE9, while AXE4 displayed even lower activity than ACE3.

The ability of AXE2 and FAE9 to act on both substrates is very interesting as CE1 enzymes are known to include acetyl xylan esterases, feruloyl esterases and enzymes with broader substrate specificity (Dilokpimol et al., 2022). The variation between the enzyme candidates therefore reflects the functional diversity commonly associated with the CE1 family (Nakamura et al., 2017).

5.2 Stability and Biochemical Characterization

Stability analysis showed that AXE2 and FAE9 retained 85-95% and 75-85% of their activity, respectively, across the approximately 20-day storage period, with only a small decrease over time. In contrast, AXE4 and ACE3 showed a more noticeable reduction, to almost 60%, in activity during storage. The higher stability found for AXE2 and FAE9 is interesting, particularly since both enzymes also showed activity towards *p*NP-acetate and *p*NP-ferulate during the screening experiments.

NanoDSF analysis also showed differences in the preferred biochemical conditions of the CE1 enzymes. Previously obtained NanoDSF data showed that AXE2 works well at a pH of 6.4, while AXE4 showed a preferred pH of 5.6, both enzymes working at 40 ℃. NanoDSF analysis performed for ACE3 and FAE9 showed preferred pH values of 5.6 and 6 respectively. FAE9 additionally showed a higher possible temperature of 50℃, whereas other enzymes had lower temperatures and hence were analyzed at 40℃.

Based on these observations, AXE2 and FAE9 were selected for the biomass substrate experiments using their respective pH and temperatures. The differences in stability, pH and temperature depict the biochemical diversity present within the CE1 family.

5.3 Kinetic Characterization

The kinetic analysis provided insight into the catalytic properties of the selected CE1 enzymes. AXE2 and FAE9 were active on both *p*NP-acetate and *p*NP-ferulate, while ACE3 only showed detectable activity toward *p*NP-acetate under the tested conditions.

AXE2 and FAE9 showed comparable kinetic behaviour toward *p*NP-acetate, with relatively low K_m values and high V_{max} values. In comparison, ACE3 showed substantially higher K_m and a lower V_{max}, indicating weaker substrate affinity and lower catalytic performance toward the acetate substrate. This reflects the lower activity that was also seen for ACE3 during the earlier screening experiments.

Differences were also present in the ferulate kinetics of AXE2 and FAE9 toward the two substrates. AXE2 showed a slightly lower K_m for *p*NP-ferulate than for *p*NP-acetate, proving good interaction with the feruloyl substrate, even though the reaction rate remained lower. In contrast, FAE9 showed a lower K_m for *p*NP-acetate than for *p*NP-ferulate, indicating a stronger affinity toward the acetyl substrate. When compared directly, AXE2 displayed a higher affinity toward *p*NP-ferulate than FAE9, whereas FAE9 showed a higher affinity toward *p*NP-acetate than AXE2. Despite the differences, both enzymes maintained activity toward both substrates, supporting broader substrate tolerance compared to other enzymes analyzed in this study.

In addition to substrate affinity, there were differences in catalytic turnover and catalytic efficiency between the enzymes. AXE2 showed stronger affinity toward *p*NP-ferulate, and FAE9 displayed a higher k_{cat} and catalytic efficiency values for both substrates, particularly *p*NP-acetate. This points towards the fact that FAE9 was able to hydrolyze the substrates more efficiently despite the differences in affinity between the enzymes. In contrast, ACE3 showed much lower catalytic efficiency, which was consistent with the lower activity detected during the functional screening assays. These results indicate that the enzymes differed not only in substrate preference, but also in their catalytic performance.

The variation between the enzymes in this study is expected, as CE1 enzymes are known to differ considerably in substrate preference and catalytic behaviour (Nakamura et al., 2017). The ability of AXE2 and FAE9 to hydrolyze both *p*NP-acetate and *p*NP-ferulate may indicate dual esterase activity. At the same time, the differences between the CE1 candidates prompt the distinct catalytic properties of these enzymes despite belonging to the same enzyme family.

5.4 Activity of CE1 Enzymes on Complex Substrates

The HPAEC-PAD analysis showed noticeable differences between the control, PP-treated and PP + enzyme samples across the different substrates analyzed. In general, treatment with Pentopan Mono BG resulted in the formation of smaller oligosaccharides, while additional changes were seen when the CE1 enzymes were present along with the GH11 xylanase. These changes included increases or decreases in specific peaks as well as the appearance or disappearance of additional peaks in some cases.

The clearest effects were seen for the arabinoxylan and xylan-containing substrates, particularly wheat arabinoxylan, rye arabinoxylan, acetylated birchwood xylan and beechwood xylan (Kulathunga et al., 2025; Knudsen et al., 2010). This is likely due to the use of G11 endoxylanase, which hydrolyses the glycosidic bonds the xylan backbone, for the synergy studies (Schmitz et al., 2022). In these substrates, increased peak areas for smaller oligosaccharides, especially xylobiose and the early-eluting peak Z, were repeated detected in the enzyme treated samples. Peak Z was prominent in several chromatograms and may correspond to small hydrolysis products such as xylose or short substituted oligosaccharides released during hydrolysis. At the same time, several larger and early-eluting peaks decreased following enzyme treatment, showing breakdown of more complex xylan-derived structures into smaller products.

This pattern was especially visible for acetylated birchwood xylan and beechwood xylan samples, where multiple late-eluting peaks showed decreasing peak areas after reaction. Since CE1 esterases are associated with the removal of acetyl and feruloyl substitutions from xylan chains, these observations may indicate deacetylation or debranching of the substrate. It is also possible that hydrolysis of the xylan backbone by Pentopan Mono exposed additional substituted regions, allowing improved access for the CE1 enzymes and contributing to the changes.

Even though both enzymes showed broadly similar hydrolysis profiles, some differences between AXE2 and FAE9 still existed. For several xylan-containing substrates, AXE2 generally resulted in stronger increases in peak Z and X2, a greater release of smaller hydrolysis products. FAE9 showed similar trends, but in some cases the changes were less pronounced.

The arabinogalactan and arabinan-rich substrates produced profiles that were simpler and differed clearly from those of the xylan-containing substrates. Larch arabinogalactan, sugar beet and acacia gum generally showed only a small number of early-eluting peaks, with one dominant peak increasing strongly in the enzyme-treated samples. Since these substrates are rich in arabinose- and galactose- containing polysaccharides, the visible peaks may correspond to smaller products containing arabinose or galactose released during the reaction (Westphal et al., 2010; Goellner et al., 2011).

Acacia gum showed a particularly distinct pattern in which peak Z increased while peak B decreased following the enzymatic reaction. Considering the highly branched arabinogalactan

structure of acacia gum, this trend may indicate partial hydrolysis of larger substituted fragments into smaller products. However, since suitable oligosaccharide standards were not available, and accurate monosaccharide estimation is not definitive with PA-200, identification of these peaks could not be performed (Mohamed et al., 2025).

The HPAEC-PAD analysis supported the findings from the findings from the functional screening and kinetic experiments. Across several complex substrates, both CE1 enzymes appeared in influence hydrolysis in the presence of Pentopan Mono. The changes also mean possible synergy between the CE1 enzymes and the GH11 xylanase, where both backbone hydrolysis and modification of substituted regions may have contributed to improved substrate degradation. Several peaks could not be definitively identified, but the repeated increase in smaller hydrolysis products along with the reduction of larger polysaccharide peaks show that these enzymes play a role in biomass degradation.

6. CONCLUSION

The enzymes analyzed in this study showed measurable differences in substrate preference and catalytic behaviour, showing the functional diversity within the CE1 family. Both AXE2 and FAE9 were active toward both model substrates, though their activities differed depending on substrate. AXE2 showed stronger affinity toward feruloyl substrate, whereas FAE9 showed higher catalytic efficiency toward *p*NP-acetate. In comparison, ACE3 displayed lower activity and appeared to prefer acetyl substrates.

The hydrolysis experiments using complex polysaccharide substrates showed that AXE2 and FAE9 influenced the chromatographic profiles generated by Pentopan Mono, particularly for the xylan-rich substrates. Increased formation of smaller oligosaccharides, with decreases in larger peaks suggests that the CE1 enzymes contributed to breakdown of substituted polysaccharide structures and improved accessibility. The results also point towards a possible synergistic relationship between the CE1 enzymes and GH11 xylanase, where side-chain modification and backbone hydrolysis may support more efficient degradation of plant biomass.

Therefore, the findings of this study support the proposed accessory role of CE1 enzymes in biomass degradation and provide insight into their potential use in enzymatic biomass conversion systems.

7. REFERENCES

Alalouf O, Balazs Y, Volkinshtein M, Grimpel Y, Shoham G, Shoham Y. **(2011).** A new family of carbohydrate esterases is represented by a GDSL hydrolase/acetylxylan esterase from Geobacillus stearothermophilus. *J Biol Chem*. 286(49):41993-42001.

Armendáriz-Ruiz M., Rodríguez-González J.A., Camacho-Ruíz R.M., Mateos-Díaz J.C. **(2018)**. Carbohydrate Esterases: An Overview. Lipases and Phospholipases. *Methods in Molecular Biology*, Vol 1835:39-68.

Brethauer S, Shahab R, Studer M. **(2020).** Impacts of biofilms on the conversion of cellulose. *Applied Microbiology and Biotechnology*. 104:5201-5212.

CAZy Database **(2026)**. Carbohydrate Esterase Family 1.

Chowdhury P, Mahi N.A, Yeassin R, Chowdhury N, Farrok O. **(2025).** Biomass to biofuel: Impacts and mitigation of environmental, health, and socioeconomic challenges. *Energy Conversion and Management: X*. Vol 25: 100889.

Dilokpimol A, Verkerk B, Li X, Bellemare A, Lavallee M, Frommhagen M, Underlin E.N, Kabel M.A, Powlowski J, Tsang A, de Vries R.P. **(2022).** Screening of novel fungal Carbohydrate Esterase family 1 enzymes identifies three novel dual feruloyl/acetyl xylan esterases. *FEBS Lett.* 596(15):1932-1943

Drula E, Garron ML, Dogan S, Lombard V, Henrissat B, Terrapon N. **(2022).** The carbohydrate-active enzyme database: functions and literature. *Nucleic Acids Res.*50(D1):D571-D577.

Francis DM, Page R. (**2010)**. Strategies to optimize protein expression in E. coli. *Curr Protoc Protein Sci*. 5(1):5.24.1-5.24.29

François Baneyx. (**1999)**. Recombinant protein expression in Escherichia coli. *Current Opinion in Biotechnology*. Vol 10, Issue 5(411-421)

Goellner EM, Utermoehlen J, Kramer R, Classen B. (**2011)**. Structure of arabinogalactan from Larix laricina and its reactivity with antibodies directed against type-II-arabinogalactans. *Carbohydrate polymers.* Vol 86, 4:1739-1744.

Grippi D, Clemente R, Bernal M.P. **(2020)**. Chemical and Bioenergetic Characterization of Biofuels from Plant Biomass: Perspectives for Southern Europe. *Appl. Sci.* 10(10), 3571.

Knudsen KEB, Laerke HN. (**2010**). REVIEW: Rye Arabinoxylans: Molecular Structure, Physicochemical Properties and Physiological Effects in the Gastrointestinal Tract. *Cereal Chemistry.* Vol 87,4:353,362.

Kulathunga J, Islam S. (**2025)**. Wheat arabinoxylans: Insight into structure-function relationships. *Carbohydrate polymers.* Vol 38, B, 122933.

Leontakianakou S, Adlercreutz P, Nordberg Karlsson E. **(2025)** Fantastic Ferulic Acid Esterases and Their Functions. *Int J Mol Sci*. 26(15):7474.

Li X, Griffin K, Langeveld S, Frommhagen M, Underlin E.N, Kabel M.A, de Vries R.P and Dilokpimol A. **(2020).** Functional Validation of Two Fungal Subfamilies in Carbohydrate Esterase Family 1 by Biochemical Characterization of Esterases From Uncharacterized Branches. *Front. Bioeng. Biotechnol*. Vol 8:694.

Mäkelä M.R, Dilokpimol A, Koskela S.M, Kuuskeri J, de Vries R.P, Hildén K. **(2018)** Characterization of a feruloyl esterase from *Aspergillus terreus* facilitates the division of fungal enzymes from Carbohydrate Esterase family 1 of the carbohydrate-active enzymes (CAZy) database. *Microb Biotechnol*. 11(5):869-880.

Megazyme **(n.d).** Xylan (Birchwood, partially acetylated).

Mohamed SA, Elsherbini AM, Alrefaey HR, Adelrehman K, Moustafa A, Egodawaththa NM, Crawford KE, Nesnas N, Sabra SA. (**2025)**. Gum Arabic: A Commodity with Versatile Formulations and Applications. *Nanomaterials (Basel).* 15(4):290.

Nakamura A.M, Nascimento A.S, Polikarpov I. **(2017).** Structural Diversity of Carbohydrate Esterases. *Biotechnology Research and Innovation.* Vol 1:35-51.

Oliveira D.M, Mota T.R, Oliva B, Segato F, Marchiosi R, Ferrarese-Filho O, Faulds C.B, Santos W.D. **(2019).** Feruloyl esterases: Biocatalysts to overcome biomass recalcitrance and for the production of bioactive compounds. *Bioresource Technology.* Vol 278:408-423.

Phienluphon A, Kondo K, Mikami B, Nagata T, Katahira M. **(2023)**. Structural insights into the molecular mechanisms of substrate recognition and hydrolysis by feruloyl esterase from *Aspergillus sydowii. International Journal of Biological Macromolecules.* Vol 253, Part 5.

Schmitz E, Leontakianakou S, Norlander S, Karlsson EN, Adlercreutz P. (**2022**). Lignocellulose degradation for the bioeconomy: The potential of enzyme synergies between xylanases, ferulic acid esterase and laccase for the production of arabinoxylo-oligosaccharides. *Bioresource Technology*. Vol 343, 126114, ISSN 0960-8524.

Westphal Y, Kuhnel S, Waard PD, Hinz SWA. (**2010)**. Branched arabino-oligosaccharides isolated from sugar beet arabinan. *Carbohydrate Research.* 345(9):1180-9.

Wu H, Xue Y, Li H, Huigan G, Liu J, Long M. **(2016).** Heterologous Expression of a New Acetyl Xylan Esterase from *Aspergillus niger* BE-2 and its Synergistic Action with Xylan-Degrading Enzymes in the Hydrolysis of Bamboo Biomass. *BioResources.* 12(1):434-447.

Yang X, Zhang Y, Sun P, Peng C. **(2024)** A review on renewable energy: Conversion and utilization of biomass. *Smart Mol*. 10;2(4):e20240019.

Yoshimi Y, Tryfona T, Dupree P. **(2024).** Structure, Modification Pattern, and Conformation of Hemicellulose in Plant Biomass. *Journal of Applied Glycoscience.* 72(1).

8. APPENDIX

8.1 Standard Curve: Bradford Assay for Protein Quantification

Table A1: BSA concentration and the absorbance values used for the preparation of the Bradford standard curve

BSA Concentration (mg/mL)	Absorbance 1 (595nm)	Absorbance 2 (595nm)	Mean Absorbance
2.0	1.068	1.079	1.074
1.8	1.047	1.044	1.046
1.6	1.014	1.030	1.022
1.4	1.005	1.001	1.003
1.2	0.960	0.953	0.957
1.0	0.880	0.854	0.867
0.8	0.757	0.752	0.755
0.6	0.600	0.609	0.605
0.4	0.436	0.435	0.436
0.2	0.214	0.218	0.216

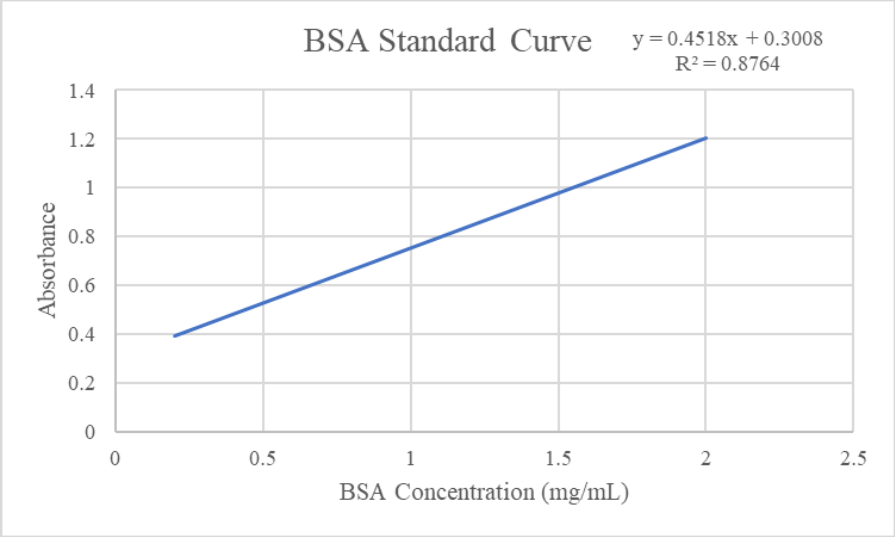

Figure A1: BSA Standard curve used for protein quantification

8.2 *p*NP standard curve used for quantification of enzymatic activity

Table A2: *p*NP concentrations and absorbance values used for the preparation of the standard curve

***p*NP Concentration (µM)**	**Absorbance**
0	0.044
50	0.092
100	0.134
200	0.223
250	0.279
300	0.323
350	0.375
400	0.415

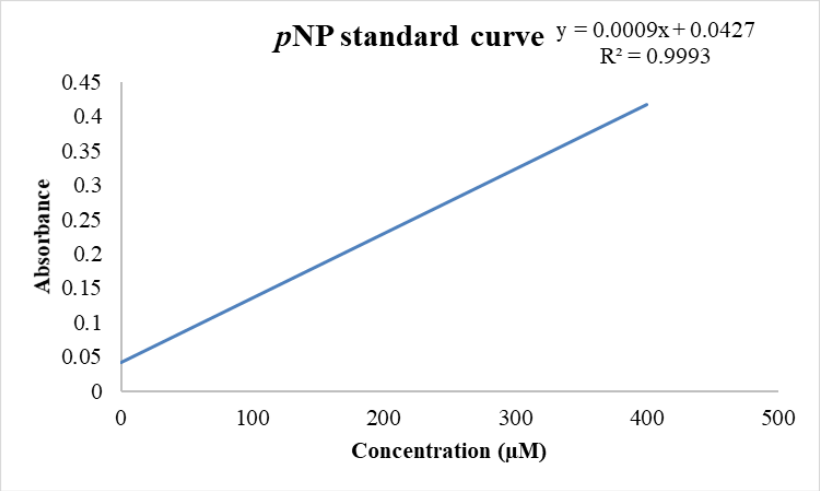

Figure A2: *p*NP Standard curve

8.3 Stability Analysis of CE1 Enzymes

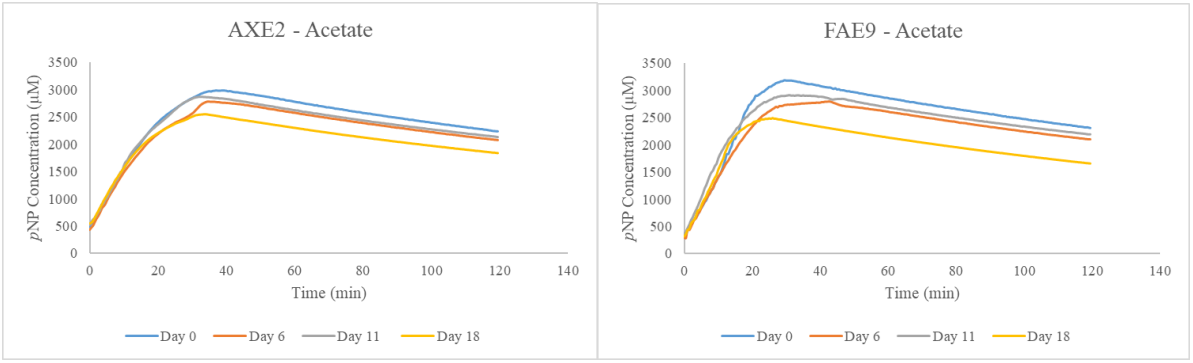

Figure A3: Representative reaction curves used for stability analysis of CE1 enzymes on *p*NP substrate.

8.4 Kinetic Characterization

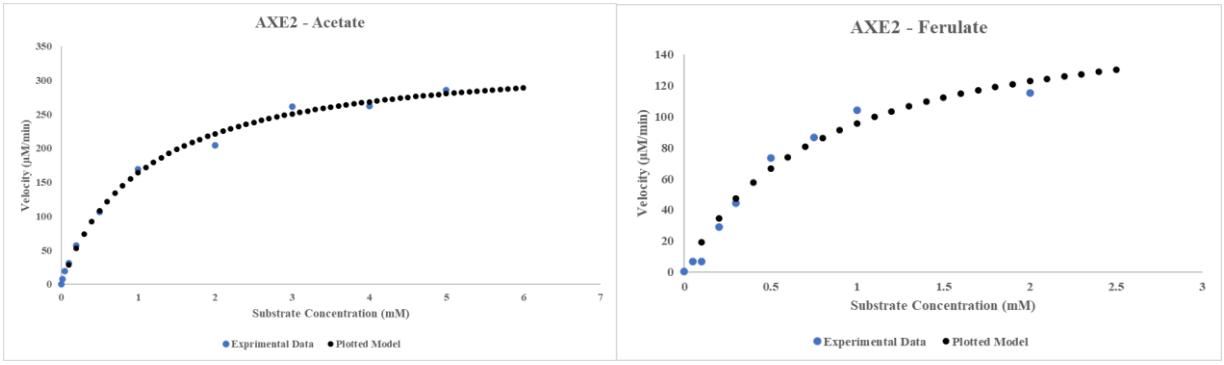

Figure A4: Representative Michaelis-Menten plots for selected CE1 enzymes

8.5 HPAEC-PAD Analysis

Table A3: Peak area values obtained from HPAEC-PAD chromatograms. All values are reported in nC*min.

Substrate	Enzyme	Peak	Control	PP	PP + Enz (t=0h)	PP + Enz (t=48h)
Wheat Arabinoxylan	AXE2	A	1.6982	2.8420	1.6727	6.0250
		X1	3.7166	7.0278	3.5303	8.6169
		X2	3.5003	1.9849	3.1023	2.3178

	FAE9	A	1.3918	3.1938	1.0337	4.6179
		X1	3.3294	7.1631	3.1695	6.6265
		X2	3.3616	1.5543	1.3552	1.6306
Rye Arabinoxylan	AXE2	A	-	2.3321	-	3.5116
		X1	-	3.8863	1.9890	3.8991
		X2	-	1.2005	1.7552	1.2549
		X5	-	0.5151	-	1.2443
	FAE9	A	-	1.7808	-	2.4084
		X1	-	2.7767	1.7405	3.6012
		X2	-	0.6127	1.3631	0.8493
		X5	-	0.2678	-	0.8288
Larch Arabinogalactan	AXE2	A	0.2597	1.2967	0.0680	3.0547
	FAE9	A	0.1411	1.6446	0.2620	3.2905
Arabinan – Sugar Beet	AXE2	A	0.3224	1.7854	0.3560	3.4555
	FAE9	A	0.4971	2.1844	0.2646	3.6893
Acetylated Xylan Birchwood	AXE2	A	3.6699	8.1566	3.7830	9.3520
		X1	6.9010	22.1342	11.4251	20.9129
		X2	6.2760	10.1320	8.8559	9.6091
		X3	5.6639	6.6976	6.6995	6.3964
		X4	4.6957	5.0651	5.4415	4.7835
		X5	3.7747	3.5667	3.9259	3.1108
	FAE9	A	6.3877	7.2567	3.7872	8.1103
		X1	11.0412	19.8123	8.6453	22.0301
		X2	8.8568	7.6150	9.0939	8.3221

		X3	7.2161	5.5955	7.0700	4.1413
		X4	6.0056	3.9218	5.6599	2.5198
		X5	5.0245	2.5267	4.1043	1.4804
Beechwood Xylan	AXE2	A	0.2335	6.0459	0.5209	7.6437
		X1	0.1385	29.4216	14.8624	26.5947
		X2	0.9252	12.0924	14.2489	9.6889
		X3	0.9502	0.5655	2.7555	1.9177
	FAE9	A	-	8.5984	0.1611	6.8542
		X1	-	32.3404	16.1429	20.0015
		X2	-	10.0935	14.7408	7.0494
		X3	-	0.6184	2.1041	0.3897
Acacia Gum	AXE2	A	0.5048	1.3738	0.5105	2.4043
		B	0.5948	0.4945	0.5183	0.4273
	FAE9	A	0.6103	2.2583	0.4179	3.3512
		B	0.7745	0.5500	0.5737	0.4244